

Circular polarization in pulsar integrated profiles

J. L. Han¹, R. N. Manchester², R. X. Xu³, and G. J. Qiao^{4,3,5}

¹*Beijing Astronomical Observatory, Chinese Academy of Sciences (CAS), Beijing 100012, China*

²*Australia Telescope National Facility, CSIRO, PO Box 76, Epping NSW 2121, Australia*

³*Department of Geophysics, Peking University (PKU), Beijing 100871, China.*

⁴*CCAT (World Laboratory), PO Box 8730 Beijing 100080, China*

⁵*Beijing Astronomy Center, CAS-PKU, Beijing 100871, China*

31 March 2018

ABSTRACT

We present a systematic study of the circular polarization in pulsar integrated profiles, based on published polarization data. For core components, we find no significant correlation between the sense-change of circular polarization and the sense of linear position angle variation. Circular polarization is not restricted to core components and, in some cases, reversals of circular polarization sense are observed across the conal emission. In conal double profiles, the sense of circular polarization is found to be correlated with the sense of position-angle variation. Pulsars with a high degree of linear polarization often have one hand of circular polarization across the whole profile. For most pulsars, the sign of circular polarization is the same at 50-cm and 20-cm wavelength, and the degree of polarization is similar, albeit with a wide scatter. However, at least two cases of frequency-dependent sign reversals are known. This diverse behaviour may require more than one mechanism to generate circular polarization.

Key words: pulsars: general — polarization

1 INTRODUCTION

From the earliest observations (e.g. Clark & Smith 1969), it has been clear that individual pulses from pulsars have high linear and circular polarization, often with a sense change of circular polarization through the pulse. The polarization distribution diagrams of Manchester, Taylor & Huguenin (1975), Backer & Rankin (1980) and Stinebring et al. (1984a,b) show clearly the variable nature of the circular polarization. Very high degrees of circular polarization are occasionally observed in individual pulses, even up to 100 per cent (Cognard et al. 1996) and mean values are typically 20 – 30 per cent.

Integrated or average pulse profiles generally have a much smaller degree of circular polarization (e.g. Lyne, Smith & Graham 1971; Manchester 1971), showing that the sign of the circular Stokes parameter V (here defined to be $I_{LH} - I_{RH}$) is variable at a given pulse phase. Significant net V is observed in the mean pulse profiles of most pulsars. In many cases, it is concentrated in the central part of the profile and shows a reversal of sense near the centre, but in other pulsars the same sense is retained throughout. It is common to identify a central peak or region of a profile as ‘core’ emission, and the outer parts as ‘conal’ emission (Rankin 1983; Lyne & Manchester 1988). Various properties, for example, spectral index, often vary from the central to the outer parts of a profile. Rankin (1983) suggested that core and conal

emissions have different emission mechanisms, with circular polarization being a property of core emission only, but Lyne & Manchester (1988) and Manchester (1995) argued that there is merely a gradation of properties across the whole emission beam. Radhakrishnan & Rankin (1990) identified two types of circular polarization: ‘antisymmetric’, in which there is a sense change near the centre of the profile, and ‘symmetric’, where the same hand of circular polarization is observed across the pulse profile. In pulsars with antisymmetric V , they found a correlation of the direction of circular sense change with the direction of linear position-angle (PA) swing.

The observed diverse circular polarization properties may relate to the pulsar emission mechanism or to propagation effects occurring in pulsar magnetosphere (cf. Melrose 1995). In the widely adopted magnetic pole models (Radhakrishnan & Cooke 1969; Komesaroff 1970; Sturrock 1971; Ruderman & Sutherland 1975), it seems very difficult to explain various circular polarization behaviours. Cheng & Ruderman (1979) suggested that the expected asymmetry between the positively and negatively charged components of the magnetoactive plasma in the far magnetosphere of pulsars will convert linear polarization to circular polarization. On the other hand, Kazbegi, Machabeli & Melikidze (1991, 1992) argued that the cyclotron instability, rather than the propagation effect, is responsible for the circular polarization of pulsars. Other authors have argued for its intrinsic origin

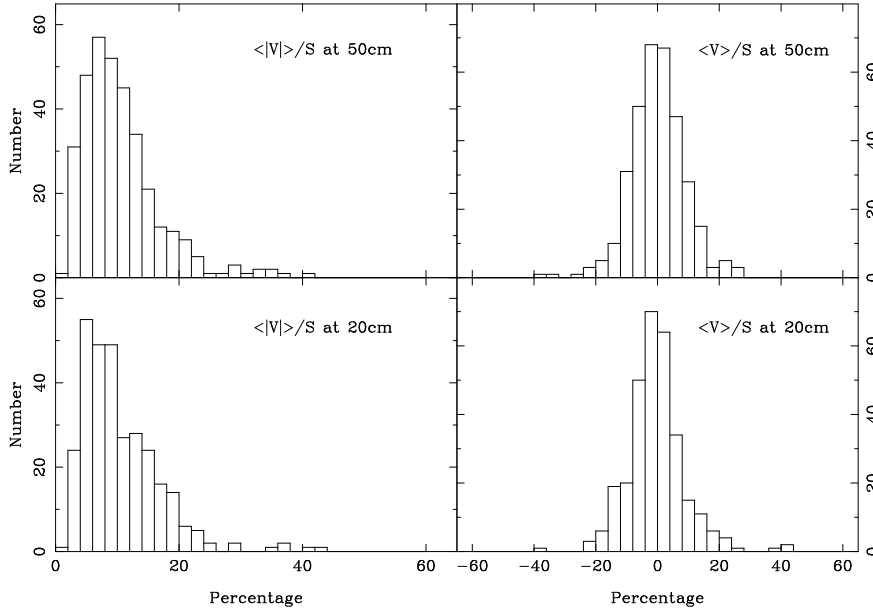


Figure 1. Distribution of $\langle |V| \rangle / S$ and $\langle V \rangle / S$ at wavelengths of 50cm and 20cm.

(Michel 1987; Gil & Snakowski 1990a,b; Radhakrishnan & Rankin 1990; Gangadhara 1997). In summary, the observed circular polarization of pulsar radiation is presently not well understood.

This paper attempts to summarize the main features of the observed circular polarization in pulsar mean pulse profiles and to discuss these in the context of other pulsar properties. We outline the main characteristics of pulsar circular polarization in Section 2, discuss possible mechanisms for the generation of circular polarization in Section 3, and present our conclusions in Section 4.

2 CIRCULAR POLARIZATION PROPERTIES

Information about circular polarization and PA variations from all available published polarization profiles is summarized in Appendix A, Table A1. Only pulsars with significant circular polarization (i.e., signal/noise in V greater than three) are included in the Table. For about 40 per cent of the pulsars examined, circular polarization is below this threshold. In the following subsections, we discuss various characteristics of the observed circular polarization.

2.1 Degree of circular polarization

Fig. 1 shows histograms of $\langle |V| \rangle / S$ and $\langle V \rangle / S$ in the 50-cm band (~ 650 MHz) and 20-cm band (~ 1400 MHz), where $S = \langle I \rangle$ is the mean flux density, for the pulsars in Table A1. Levels of circular polarization are very similar at the two wavelengths; the median value of $\langle |V| \rangle / S$ is 9 per cent at 50 cm and 8 per cent at 20 cm. Only a few pulsars have mean circular polarization exceeding 20 per cent. The apparent deficit of pulsars with $\langle |V| \rangle / S \lesssim 5$ per cent is not real; for low signal/noise observations, noise in the profile makes a positive contribution to $\langle |V| \rangle / S$. Although the least significant signal/noise ratios in V were not included in the

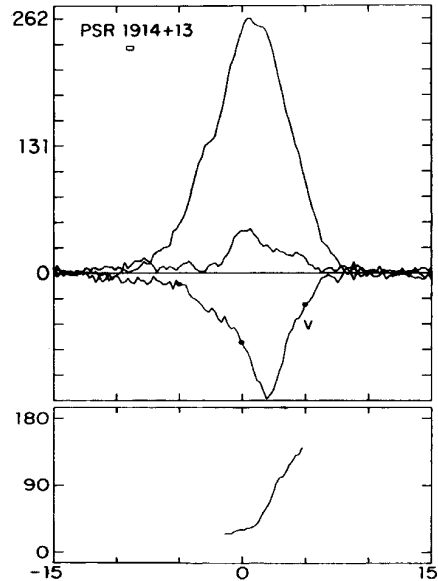


Figure 2. Polarization profile for PSR B1914+13, a pulsar with strong circular polarization over the whole observed profile (From Rankin, Stinebring & Weisberg 1989).

sample, many of the profiles have relatively low signal/noise ratio and hence a biased estimate of $\langle |V| \rangle / S$.

As Fig. 1 shows, strong circular polarization has been detected from only a small number of pulsars; an example of such a pulsar is shown in Fig. 2. Pulsars with $\langle |V| \rangle / S > 20$ per cent and polarization error < 5 per cent are listed in Table 1. PSR B1702–19, an interpulse pulsar, has the highest known fractional circular polarization, up to 60 per cent (Biggs et al. 1988); note, however, that Gould (1994) gives values of 30 – 35 per cent. PSR B1914+13, a pulsar with almost the same P and \dot{P} , and hence the same estimates of characteristic age, surface magnetic field and total energy-

Table 1. Pulsars with strong circular polarization

| PSR | Freq. (MHz) | $\langle V \rangle/S$ (%) | $\langle V\rangle/S$ (%) | $\langle L\rangle/S$ (%) | Err. (%) | Ref. |
|------------|----------------|------------------------------|-----------------------------|-----------------------------|-------------|----------|
| B1702-19 | 408 | 60 | -60 | 35 | 2 | B88 |
| B1913+10 | 1400 | 38 | 38 | 35 | 2 | R89 |
| B1914+13 | 1400 | 37 | -37 | 18 | 2 | R89 |
| B0835-41 | 405 | 35 | 35 | 3 | 3 | H77 |
| B1221-63 | 950 | 33 | 26 | 30 | 5 | Mc78,v97 |
| B1557-50 | 1612 | 23 | 21 | 11 | 4 | Ma80 |
| B0942-13 | 408 | 23 | 19 | 22 | 1 | G94 |
| J1359-6038 | 660 | 22 | 22 | 83 | 2 | M98 |
| B2327-20 | 648 | 22 | -22 | 16 | 1 | Mc78 |
| B1737-30 | 1560 | 22 | -22 | 87 | 3 | W93 |
| B1952+29 | 1400 | 21 | -19 | 18 | 1 | R89 |
| B1857-26 | 1612 | 20 | -1 | 23 | 3 | Ma80 |

References: Hamilton et al. 1977 (H77); McCulloch et al. 1978 (Mc78); Manchester, Hamilton & McCulloch 1980 (Ma80); Biggs et al. 1988 (B88); Rankin, Stinebring & Weisberg 1989 (R89); Wu et al. 1993 (W93); Gould 1994 (G94); van Ommen et al. 1997 (v97); Manchester, Han & Qiao 1998 (M98).

Table 2. Circular sign reversals and sign of PA variation.

| LH/RH = +/- | | RH/LH = -/+ | |
|-------------|-------------|-------------|------------|
| PA: dec | PA: inc | PA: dec | PA: inc |
| B1237+25 | B0823+26m | B0329+54 | B0450-18 |
| B1508+55 | J1001-5507? | J0437-4715 | B1700-32 |
| B1737+13 | J1604-4909 | B0942-13 | J2144-3933 |
| J1801-0357? | B2002+31 | B1323-58 | |
| B1821+05? | B2003-08 | B1451-68 | |
| B1857-26 | B2113+14 | J1527-5552 | |
| B1859+03 | | B1534+12 | |
| B2045-16 | | J1852-2610 | |
| B2111+46 | | B1907+02 | |

For PSRs B1821+05, J1801-0357 and J1001-5507, the PA variation is not very clear.

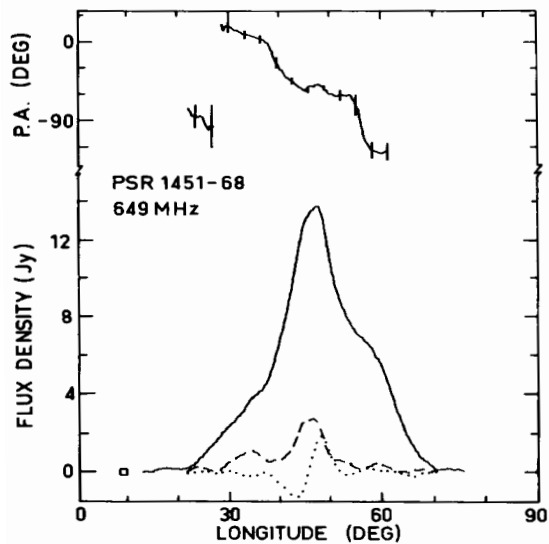
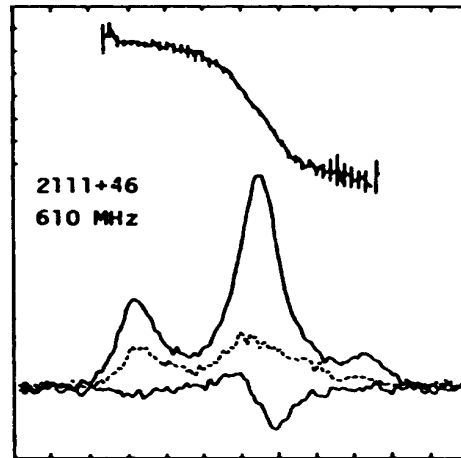
loss rate \dot{E} as PSR B1702-19, also has very strong circular polarization (Fig. 2).

As Table 1 shows, all but one of the pulsars with strong circular polarization is symmetric, i.e., with no reversals of V across the pulse profile. These pulsars are discussed further in Section 2.4 below. Although most of these pulsars also have relatively high levels of fractional linear polarization, a few do not.

2.2 Antisymmetric circular polarization and core emission

As mentioned in Section 1, circular polarization is often stronger in the central or core regions of a profile, and often shows a reversal in sign near the profile centre. From a sample of 25 pulsars, Radhakrishnan & Rankin (1990) found a correlation between the sense of the sign reversal and the sense of PA swing, with transitions of circular polarization from LH to RH (+/-) being associated with decreasing PA (clockwise rotation on the sky) across the profile, and vice versa. The proposed correlation was questioned by Gould (1992, 1994) who found some contrary examples.

Table 2 lists pulsars with a reversal in the sign of V

**Figure 3.** Two examples of pulsars with central reversals in the sign of V . (From Lyne & Manchester 1988 and McCulloch et al. 1978)

in the central or core region of the profile, and two good examples are shown in Fig. 3. In Table 2, pulsars are divided into different columns according to the sense of the V sign change and the direction of PA swing. Further information about the observations can be found in Table A1. Among 27 pulsars listed, 12 pulsars (in the first and fourth columns) agree with the correlation proposed by Radhakrishnan & Rankin (1990) and 15 pulsars (in the second and third columns) disagree. We therefore conclude that there is no correlation between the sense of the sign change of circular polarization and the sense of variation of linear polarization angle across the profile. Consequently, theoretical discussions based on this correlation (e.g. Radhakrishnan & Rankin 1990; Kazbegi et al. 1991) are not well founded.

It is worth noting that central or 'core' reversals in circular polarization sense usually occur very close to the mid-point of the pulse profile and do not appear to be related to any particular peak in the total intensity profile. For example, PSR B0149-16 at 50 cm (Qiao et al. 1995) has a central reversal in V between two overlapping pulse

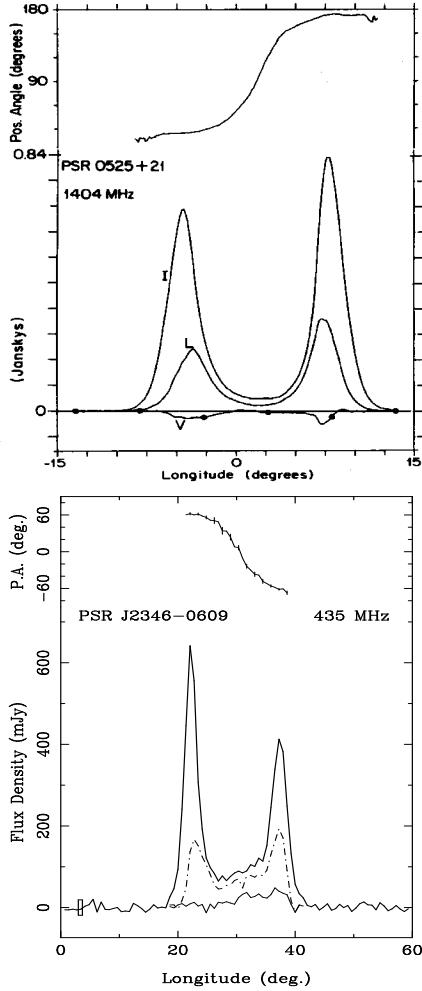


Figure 4. Two examples of conal-double pulsars with significant circular polarization. (From Stinebring et al. 1984a and Manchester, Han & Qiao 1998)

components; PSRs B1855+09 (main pulse) and B1933+16 (Segelstein et al. 1986; Rankin et al. 1989) are similar. In other pulsars, e.g. PSRs B1451–68 and B2003–08, the central peak is offset in longitude from the profile mid-point. Some conal double pulsars, such as PSR B2048–72, have a clear central reversal but no core component at all. These observations suggest that the ‘core’ sense reversal is associated with the central region of the beam, rather than with any particular component.

2.3 Circular polarization in cone-dominated pulsars

It is often stated that the conal components of pulsar profiles have weak or no circular polarization (e.g. Radhakrishnan & Rankin 1990; Gil et al. 1995). However, there are many examples of significant circular polarization in profiles, or parts of profiles, which are believed to be conal emission. Fig. 4 shows two ‘conal-double’ pulsars which show significant circular polarization.

In most cases, the circular polarization is symmetric, i.e., it has the same sign over the profile. In Table 3, we show the relationship between the sign of PA variation and sense

Table 3. Conal-double pulsars with significant circular polarization.

| PSR | PA | Sign of V | | Ref. |
|------------|-----|-------------|--------|--------------|
| | | Comp 1 | Comp 2 | |
| B0148–06 | inc | – | – | LM88 |
| B0525+21 | inc | – | – | S84a,R83 |
| B0751+32 | inc | – | – | R89 |
| B0818–13 | inc | – | – | v97,Q95,B87 |
| B0834+06 | inc | – | – | Mc78,S84a |
| | | +/- | – | S84b |
| B1133+16 | inc | – | – | Mc78,S84a |
| B1913+16 | inc | -/+ | – | C90 |
| B2020+28 | inc | +/- | – | C78,S84a |
| B2044+15 | inc | – | – | G94 |
| B2048–72 | inc | ± | ∓ | Q95,M98 |
| B0301+19 | dec | + | + | R83,R89 |
| J0631+1036 | dec | + | + | Z96 |
| B1039–19 | dec | -/+ | + | LM88,G94 |
| J1123–4844 | dec | + | + | M98 |
| B1259–63 | dec | + | · | MJ95 |
| J1527–3931 | dec | + | + | M98 |
| B1727–47 | dec | + | · | H77,Mc78,v97 |
| J1751–4657 | dec | -/+ | + | M98 |
| B2321–61 | dec | + | · | Q95 |
| J2346–0609 | dec | · | + | M98 |

References: Hamilton et al. 1977 (H77); Cordes, Rankin & Backer 1978 (C78); McCulloch et al. 1978 (Mc78); Rankin 1983 (R83); Stinebring et al. 1984a (S84a); Stinebring et al. 1984b (S84b); Biggs et al. 1987 (B87); Lyne & Manchester 1988 (LM88); Rankin, Stinebring & Weisberg 1989 (R89); Cordes, Wasserman & Blaskiewicz 1990 (C90); Gould 1994 (G94); Manchester & Johnston 1995 (MJ95); Qiao et al. 1995 (Q95); Zepka, Cordes & Wasserman 1996 (Z96); van Ommen et al. 1997 (v97); Manchester, Han & Qiao 1998 (M98).

of circular polarization in conal-double pulsars. A striking conclusion is that there is a strong correlation between these two properties, with right-hand (negative) circular polarization accompanying increasing PA and vice versa. No good examples contrary to this trend have been found. Therefore, unlike the correlation between the sense of sign change in core emission and PA swing, this correlation appears to be significant.

In some cases, a change in the sign of V is observed, generally associated with the first component. Exceptions are PSR B2048–72, where it is centrally located, and PSR B0329+54 in its ‘abnormal’ mode, where there is a sense change in the trailing conal component (Xilouris et al. 1995). Note also that, for PSR B0834+06, there is a sign change under the first component at 800 MHz, but not at 1404 MHz (Stinebring et al. 1984a,b).

In summary, these observations show that circular polarization and sense changes are not associated with any particular ‘core’ component. The implication is that there is no fundamental difference between core and conal emission.

2.4 Symmetric circular polarization

For a number of pulsars, we see one hand of circular polarization over the whole profile, the so-called ‘symmetric’ type by Radhakrishnan & Rankin (1990). Table 4 lists pul-

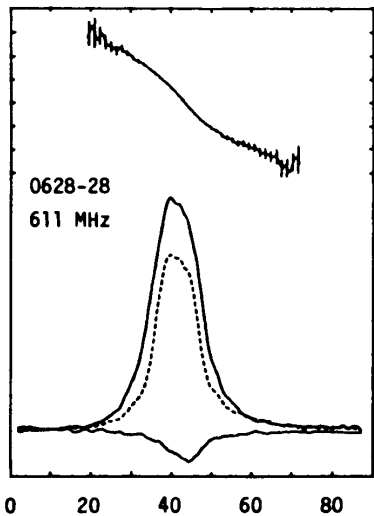


Figure 5. PSR B0628–28, an example of a pulsar with ‘symmetric’ circular polarization and high linear polarization. (From Lyne & Manchester 1988)

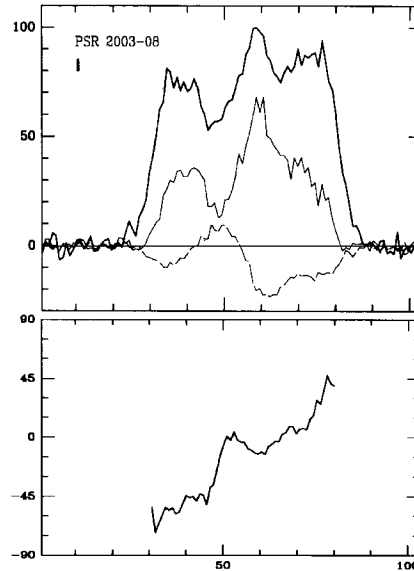


Figure 6. PSR B2003–08, a pulsar showing both symmetric and antisymmetric circular polarization. (From Xilouris et al. 1991)

Table 4. Pulsars with symmetric circular polarization

| LH = + | | RH = - | |
|------------|-----------|------------|-----------|
| PA: inc | PA: dec | PA: inc | PA: dec |
| B0611+22 | B1913+10? | J0134–2937 | B0538–75? |
| B0835–41 | | J1603–5657 | B0540+23 |
| J0942–5657 | | B1706–14 | B0628–28 |
| J1202–5820 | | B1914+13 | B0740–28 |
| J1253–5820 | | B2315+21 | B0833–45 |
| J1359–6038 | | B2327–20 | B0950+08 |
| J1722–3712 | | | B1629–50? |
| | | | B1702–19m |
| | | | B1702–19i |
| | | | B1737–30 |
| | | | B1915+13 |
| | | | B1937–26 |

sars of this type; see Table A1 for more observation details and references. Most of these pulsars have one component or several unresolved components, and a large majority have strong linear polarization. A good example, PSR B0628–28, is shown in Fig. 5.

It is worth mentioning that receiver cross-coupling can result in spurious circular polarization in strongly linearly polarized sources (e.g. Rankin & Benson 1981; Thorsett & Stinebring 1990). However, we believe that this is not relevant for most of the pulsars listed here, and hence that the correlation of symmetric circular polarization with strong linear polarization is real.

The emission from these pulsars is probably conal, either from a grazing cut of the emission beam (as in PSR B0628–28), or from a leading or trailing component. Many of these pulsars are in the young and highly polarized class identified by Manchester (1996) as having very wide conal beams. As shown above, conal-double pulsars, for which the emission comes from beam edge, generally have a single sense of circular polarization over each component. However, Table 4 shows that the correlation between sign of V

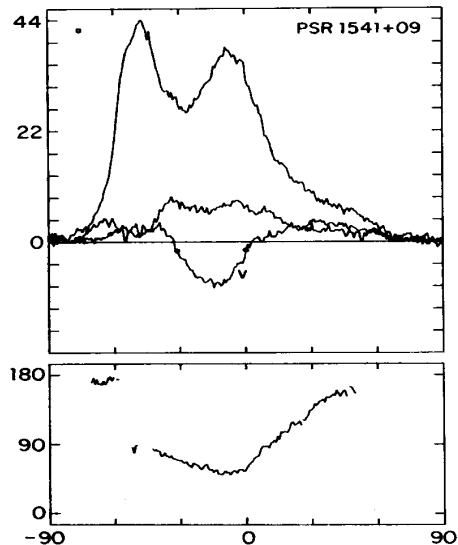


Figure 7. PSR B1541+09, a pulsar with a complex variation of circular polarization across the profile. (From Rankin et al. 1989)

and sense of PA swing observed in conal-double pulsars is not seen in the symmetric- V pulsars.

2.5 Complex variations of circular polarization with longitude

As described above, circular polarization from central or core regions of the profile is usually antisymmetric, whereas that from conal regions is usually symmetric. In some pulsars, e.g. PSR B2003–08 (Fig. 6) these two properties are superimposed, resulting in a more complex pattern of V sign changes across the profile.

Complex variations, possibly related to different com-

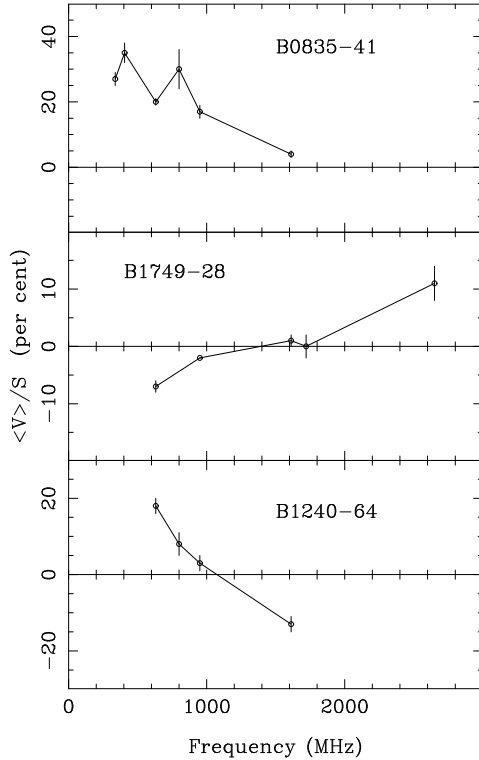


Figure 8. Frequency dependence of $\langle V \rangle / S$ for three pulsars

ponents of the profile, are seen in PSR B1541+09 (Fig. 7) and PSR B1952+29 (Rankin et al. 1989). PSR B1907+10 (Rankin et al. 1989) has relatively strong RH circular polarization, apparently related to one component of the profile.

Without doubt, the most complex variation of circular (and linear) polarization known is seen in PSR J0437–4715 (Navarro et al. 1997). As with many other pulsars, circular polarization is strongest near the main central peak of the profile and has a sign reversal at or near the profile centre. However, circular polarization is detected over most of the very wide pulse profile, with several sense reversals at other longitudes. On the leading side of the profile, these reversals may be centred on pulse components, but this is not the case on the trailing side.

2.6 Frequency dependence of circular polarization

As discussed in Section 2.1, there is little systematic difference in the degree of circular polarization between frequencies of 650 MHz (50 cm) and 1400 MHz (20 cm). This is further illustrated in Fig. 9 which shows the distributions of ratios of $\langle |V| \rangle / S$ and $\langle V \rangle / S$ at 50 and 20 cm. In both cases, the distributions are centred on 1.0 (in fact, the median value of $[\langle |V| \rangle / S]_{50} / [\langle |V| \rangle / S]_{20}$ is exactly 1.0), showing that there is little or no systematic variation in degree of circular polarization with frequency.

However, these histograms do have a wide spread. A significant number of $[\langle V \rangle / S]_{50} / [\langle V \rangle / S]_{20}$ values are negative, implying a change in sign of $\langle V \rangle$ with frequency. Fig. 8 shows the frequency dependence of $\langle V \rangle / S$ in more detail for three pulsars. For two of these, there is clear evidence for a change in sign of $\langle V \rangle$.

Table 5. Pulsars showing frequency-dependent circular polarization

| PSR | low ν | high ν | Ref. |
|----------|-----------|------------|--------------------|
| B0148–06 | – | none? | LM88,W93 |
| B0149–16 | +– | none? | Q95,X91 |
| B0355+54 | weak | strong | LM88,X91,X95 |
| B0833–45 | weak | strong | H77,Ma80,KD83 |
| B0834+06 | + / – – | – + – | S84ab,v97,Ma80 |
| B0835–41 | strong | weak | H77,Mc78,Ma80 |
| B0932–52 | – | +? | v97,M98 |
| B1240–64 | + | – | Mc78,v97,Ma80 |
| B1641–68 | strong | none? | Q95,v97,W93 |
| B1700–32 | none? | – / + | LM88,Ma80 |
| B1727–47 | weak | none? | H77,Mc78,v97,Ma80 |
| B1749–28 | – | – / + | Mc78,v97,Ma80,Mr81 |
| B2048–72 | + / – | – / + | Q95 |

References: Hamilton et al. 1977 (H77); McCulloch et al. 1978 (Mc78); Manchester, Hamilton & McCulloch 1980 (Ma80); Morris et al. 1981 (Mr81); Krishnamohan & Downs 1983 (KD83); Stinebring et al. 1984a (S84a); Stinebring et al. 1984b (S84b); Lyne & Manchester 1988 (LM88); Xilouris et al. 1991 (X91); Wu et al. 1993 (W93); Qiao et al. 1995 (Q95); Xilouris et al. 1995 (X95); van Ommen et al. 1997 (v97); Manchester, Han & Qiao 1998 (M98).

Table 5 lists pulsars with apparently significant frequency-dependent circular polarization. In some cases, such as those shown in Fig. 8, there seems no doubt about the reality of the frequency dependence. In other cases, further observations are required to establish these trends with more certainty. Simultaneous dual-frequency observations would be especially interesting.

3 DISCUSSION

We have presented a summary of all published observations relating to circular polarization of pulsar mean pulse profiles. We emphasize that we have not considered polarization of individual pulses. While individual pulse polarization may be closely related to the generation process, published results are not as complete and the properties are very variable, making analysis difficult. In general, characteristics of the mean pulse profile are stable in time, and hence provide a framework for understanding the processes related to generating the polarization.

Generally, in astronomy, wherever there is appreciable asymmetry, there is likely to be polarization at some level (Tinbergen 1996, p.27). If the asymmetry is of a scalar kind (e.g. a longitudinal component of the magnetic field), the polarization or birefringence will be circular and scalar in character. If the asymmetry is of a vector type (e.g. a transverse magnetic component), the polarization or birefringence will be linear and vector in character.

For pulsars, the radio emission is believed to be generated by highly relativistic particles moving along magnetic field lines above the magnetic poles. These field lines are curved, giving the asymmetry a vector component which, from the general principle above, results in linear polarization as in the widely accepted rotating-vector model (Radhakrishnan & Cooke 1969). There are strong curved magnetic fields, not only in the emission region, but also along

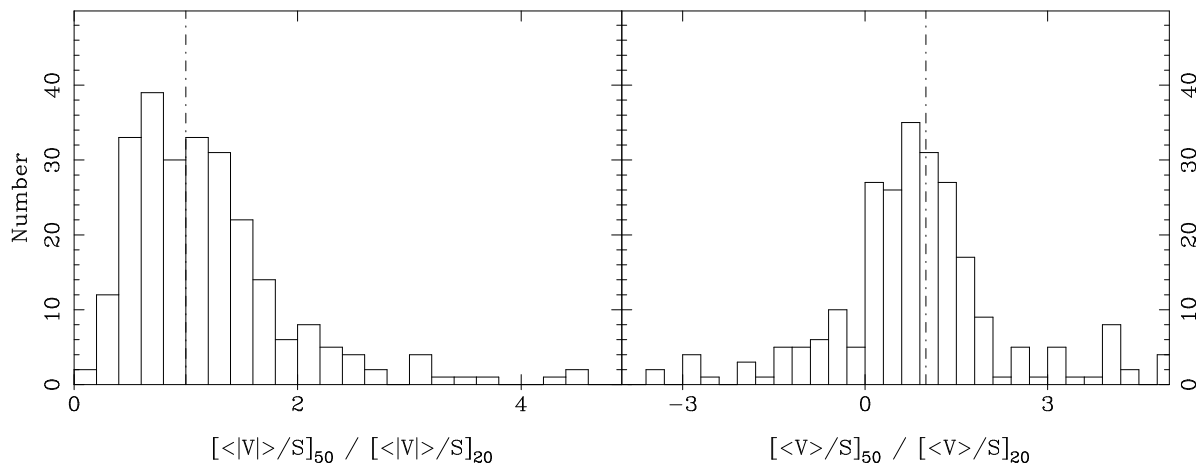


Figure 9. Distribution of ratios of $\langle|V|\rangle/S$ and $\langle V\rangle/S$ at wavelengths of 50 cm and 20 cm. The dot-dashed line marks a ratio of 1.0.

the path in the pulsar magnetosphere through which the radiation propagates. The emission region is very probably asymmetric and the emission beam is anisotropic. Hence, the observed circular polarization can be either intrinsic to the emission process or due to propagation effects, or perhaps both.

3.1 Intrinsic origin?

If the observed circular polarization is intrinsic to the emission region or radiation process, the radiation should suffer negligible modification by propagation effects. With one or two possible exceptions, the sense-reversal of circular polarization seen in central or core regions of pulsar profiles is not frequency-dependent, which suggests that the circular polarization does not arise from a propagation effect or plasma emission process (Michel 1987; Radhakrishnan & Rankin 1990). An origin related to asymmetry in the beam shape seems more likely.

If the extent of the radio emission beam is determined by the last open magnetic field lines from the polar cap, it is axisymmetric for an aligned rotator. However, the axisymmetry is broken for oblique rotators. For purely geometric reasons, the beam is elongated in the longitude direction (Biggs 1990; Roberts & Sturrock 1972).

Michel (1987) suggested that the currents out of a polar cap should preferentially flow along the shortest open field lines to the light cylinder and argued that pulsar radiation is not from a complete hollow cone, but is concentrated in the half-cone at lower latitude. In contrast, in the model developed by Arons and co-workers (e.g. Arons 1983), relativistic charged particles accelerate within the flux tubes of “favourable curvature” which bend towards the rotation axis. Pulsar emission then is only possible from the upper half beam at high latitudes.

If the pulsar radio beam is randomly patchy in structure as suggested by Lyne & Manchester (1988) and emission is generated by relativistic particles flowing along random flux tubes, then other asymmetries will be present. The fact that multiple and asymmetric components are observed in pulse profiles shows that such asymmetries exist. These may, for example, account for the complex longitude variation

of pulsar circular polarization seen in pulsars such as PSR J0437–4715.

Radhakrishnan & Rankin (1990) suggested that the elliptical shape of the pulsar beam is responsible for the antisymmetric polarization for core components. According to this model, the circular polarization should be intrinsically antisymmetric and frequency-independent. Radhakrishnan & Rankin (1990) argued that this mechanism could produce the correlation between sense change and PA variation. However, as discussed in Section 2.2, this correlation is no longer observed, indicating a different origin for the circularly polarized emission.

Gangadhara (1997) has suggested that positrons and electrons emit orthogonally polarized emission as they move along curved magnetic field lines. If the trajectories of the two species are different, coherent superposition of the two orthogonal modes would result in antisymmetric circular polarization.

3.2 Propagation effect or plasma process?

In a relativistic electron-positron plasma, for $\theta \ll 1$, $\omega_p^2/\omega_B^2 \ll 1$ and $\Delta\gamma/\gamma_p \ll 1$, two circularly polarized waves can exist if

$$\theta^2 \ll \theta_0^2 \equiv (\omega/8\omega_B)(\Delta\gamma/\gamma_p^4)$$

and two linear polarization waves can exist in the opposite case, i.e. $\theta^2 \gg \theta_0^2$ (Shafranov 1967; Kazbegi et al. 1991, 1992). Here, $\omega_B = eB/mc$, $\omega_p^2 = 4\pi n e^2/m$, θ is the angle between the wave vector and the local magnetic field direction, and γ_p is the average Lorentz factor of the plasma. The average difference, $\Delta\gamma$, of Lorentz factors for e^\pm plays a critical role in the polarization properties. If $\Delta\gamma$ is very small so that $\theta^2 \gg \theta_0^2$ is always satisfied, then we have only linear polarization modes. Conversely, when the distributions of electrons and positrons are significantly different, circular polarization waves can exist and propagate in the region of $\theta^2 \ll \theta_0^2$. This concurs with the simple principle that circular polarization is related to the longitudinal magnetic field, and allows circular polarization to propagate near the magnetic axis where the angle between the wave vector and the magnetic field can be always small.

Cheng & Ruderman (1979) introduced the term “adiabatic walking” to describe the slow change in the polarization properties during propagation in the pulsar magnetosphere. This effect can result in 100 per cent linearly polarized wave modes even when the generated waves have random polarization. In the far magnetosphere, the conditions for adiabatic walking no longer apply, and circularly polarized modes can be generated. Two distinct mechanisms were discussed. One applies to a symmetric e^\pm plasma, i.e., the positrons and electrons have the same distribution of Lorentz factors. Adiabatic walking fails near the light cylinder if the propagation direction and magnetic field are no longer coplanar; the initially linearly polarized modes then become elliptical. The second mechanism is for an asymmetric plasma. The normal modes become elliptical when the inequality $\omega \ll \gamma(eB/mc)$ is no longer satisfied because of diminishing B . Significant circular polarization can be generated before adiabatic walking ceases, so long as the curvature of field lines is sufficiently small. Cheng & Ruderman (1979) believe that this second mechanism is likely to be more significant.

Both mechanisms predict a frequency dependence of circular polarization, with weaker polarization at higher frequencies. As discussed in Section 2.6, this is seen in some pulsars, but is not generally the case. Observations over a wider frequency range would be useful.

The region of cyclotron resonance, typically located several hundred neutron-star radii above the surface, is an interesting region, where

$$|\omega_B|/\gamma = \omega(1 - \beta \cos \theta) \simeq \omega(\theta^2 + \gamma^{-2})/2.$$

Here $\beta = v/c$ for the particles. Kazbegi et al. (1991) suggested that pulsar emission is generated in this region via the cyclotron instability. For large θ , the emission is linearly polarized, but for small θ it is circularly polarized with sense corresponding to the charge signs. Net circular polarization can be produced by a relativistic electron-positron plasma with $\Delta\gamma \neq 0$. This mechanism would be expected to produce circular polarization predominantly in the central or core regions of the profile.

Propagation through this region may alter the polarization state of a wave. Istomin (1992) suggested that incident linearly polarized waves become circular as a result of generalized Faraday rotation in this region. Radiation with a wave vector in the plane of the field line (O-mode) becomes LH polarized and that with a wave vector normal to the plane (E-mode) becomes RH polarized. The two circular modes have different group velocities which could result in net circular polarization in the observed radiation. This is a possible origin for ‘symmetric’ circular polarization observed in conal emission (Table 4).

4 CONCLUSIONS

We have shown that, in pulsars, circular polarization is common but diverse in nature. It is generally strongest in the central or ‘core’ regions of a profile, but is by no means confined to these regions. The circular polarization often changes sense near the middle of the profile, but sign changes are occasionally observed at other longitudes. Relatively strong circular polarization of one hand is often observed in

pulsars which also have high linear polarization. Although examples of both increasing and decreasing degree of circular polarization with frequency, and even changes of sign, are observed, on average there is no systematic frequency dependence of polarization degree. The correlation between circular polarization sense and sense of PA swing for conal-double pulsars is very intriguing.

It seems unlikely that these diverse behaviours can be accounted for by a single mechanism for generation of circular polarization. Both intrinsic emission and propagation effects seem possible. Antisymmetric circular emission could result from asymmetries in the emission beam or from propagation effects in the pulsar magnetosphere. Confirmation of its frequency independence would support an intrinsic process. On the other hand, the strong symmetric polarization observed in conal components is most probably generated by a propagation process.

Further observations of the polarization of both individual and mean pulse profiles will help to clarify many of these issues. In particular, observations over a wide frequency range would be valuable in sorting out the importance of propagation effects.

ACKNOWLEDGMENTS

We thank Ye Jun for assistance in compiling the data presented in this paper, Dr. Dan Stinebring for permission to reproduce Fig. 2, 4a, & 7 from his papers published in ApJ, and Prof. J. Lequeux for permission to reproduce Fig. 6 from A&A. JLH thanks the Su-Shu Huang Research Foundation for support for travel to ATNF in 1996 January, where this work was initiated, and acknowledges financial support from the National Natural Science Foundation (NNSF) of China and the Research Foundation of Astronomical Committee of CAS. GJQ thanks the NNSF of China for support for his visits at ATNF and acknowledges financial support from the Climbing Project – the National Key Project for Fundamental Research of China. JLH and GJQ acknowledge support from the Bilateral Science and Technology Program of the Australian Department of Industry, Science and Tourism.

REFERENCES

- Arons J., 1983, ApJ 266, 215
- Arzoumanian Z., Phillips J.A., Taylor J.H., Wolszczan A., 1996, ApJ 470, 1111 (A96)
- Backer D.C., Rankin J.M., 1980, ApJS 42, 143 (BR80)
- Barter N., Morris D., Sieber W., Hankins T., 1982, ApJ 258, 776 (B82)
- Biggs J.D., 1990, MNRAS 245, 514
- Biggs J.D., McCulloch P.M., Hamilton P.A., Manchester R.N., Lyne A.G., 1985, MNRAS 215, 281 (B85)
- Biggs J.D., McCulloch P.M., Hamilton P.A., Manchester R.N., 1987, MNRAS 228, 119 (B87)
- Biggs J.D., Lyne A.G., Hamilton P.A., McCulloch P.M., Manchester R.N., 1988, MNRAS 235, 255 (B88)
- Cheng A.F., Ruderman M.A., 1979, ApJ 229, 348
- Clark R.R., Smith F.G., 1969, Nature 221, 724
- Cognard I., Shrauner J.A., Taylor J.H. & Thorsett S.E., 1996, ApJ 457, L81
- Cordes J.M., Rankin J.M., Backer D.C., 1978, ApJ 223, 961 (C78)

- Cordes J.M., Wasserman I., Blaskiewicz M., 1990, ApJ 349, 546 (C90)
- Costa M. E., McCulloch P. M. & Hamilton P.A., 1991, MNRAS 252, 13 (C91)
- Fruchter A.S., Berman G., Bower G., et al., 1990, ApJ 351, 642 (F90)
- Gangadhara R.T., 1997, A&A, 327 155
- Gil J.A., Snakowski J.K., 1990a, A&A 234, 237
- Gil J.A., Snakowski J.K., 1990b, A&A 234, 269
- Gil J.A., Kijak J., Maron O., Sendyk M., 1995, A&A 301, 177
- Gould D.M., 1992, in Hankins T. H., Rankin J. M., Gil J. A., eds, The magnetosphere structure and emission mechanism of radio pulsars, Proc. IAU Coll. 128, p. 384
- Gould D.M., 1994, PhD thesis, University of Manchester
- Hamilton P.A., McCulloch P.M., Ables J.G., Komesaroff M.M., 1977, MNRAS 180, 1 (H77)
- Istomin Ya. N., 1992, in Hankins T. H., Rankin J. M., Gil J. A., eds, The magnetosphere structure and emission mechanism of radio pulsars, Proc. IAU Coll. 128, p. 375
- Kazbegi A.Z., Machabeli G.Z., Melikidze G.J., 1991, MNRAS 253, 377
- Kazbegi A.Z., Machabeli G.Z., Melikidze G.J., 1992, in Hankins T. H., Rankin J. M., Gil J. A., eds, The magnetosphere structure and emission mechanism of radio pulsars, Proc. IAU Coll. 128, p. 373
- Komesaroff M.M., 1970, Nature 225, 612
- Krishnamohan S. & Downs G.S., 1983, ApJ 265, 372 (KD83)
- Lyne A.G., Manchester R.N., 1988, MNRAS 234, 477 (LM88)
- Lyne A.G., Smith F.G., Graham D.A., 1971, MNRAS 153, 337
- Manchester R.N., 1971, ApJS 23, 283 (M71)
- Manchester R.N., 1995, J. Ap&A 16, 107
- Manchester R.N., 1996, in Johnston S., Walker M. A. Bailes M., eds, Pulsars: Problems and Progress, IAU Colloquium 160. Astron. Soc. Pacific, San Francisco, p. 193
- Manchester R.N., Han J.L., Qiao G.J., 1998, MNRAS 295, 280 (M98)
- Manchester R.N., Hamilton P.A., McCulloch P.M., 1980, MNRAS 192, 153 (Ma80)
- Manchester R.N., Johnston S., 1995, ApJ 441, L65 (MJ95)
- Manchester R.N., Taylor J.H., Huguenin G.R., 1975, ApJ 196, 83
- McCulloch P.M., Hamilton P.A., Manchester R.N., Ables J.G., 1978, MNRAS 183, 645 (Mc78)
- Melrose D.B., 1995, J. Astrophys. Astr. 16, 137
- Michel F.C., 1987, ApJ 322, 822
- Morris D., Graham D.A., Sieber W., Bartel N., Thomasson P., 1981, A&AS 46, 421 (Mr81)
- Navarro J., Manchester R.N., Sandhu J.S., Kulkarni S.R., & Bailes M., 1997, ApJ, 486, 1019 (N97)
- Phillips J.A., 1990, ApJ 361, L57 (P90)
- Qiao G.J., Manchester R.N., Lyne A.G., Gould D.M., 1995, MNRAS 274, 572 (Q95)
- Radhakrishnan V., Cooke D.J., 1969, Ap letters 3, 225
- Radhakrishnan V., Rankin J.M., 1990, ApJ 352, 258
- Rankin J.M., 1983, ApJ 274, 333 (R83)
- Rankin J.M., Benson J.M., 1981, AJ 86(3), 418 (RB81)
- Rankin J.M., Stinebring D.R., Weisberg J.M., 1989, ApJ 346, 869 (R89)
- Rankin J.M., Wolszczan A., Stinebring D.R., 1988, ApJ 324, 1048 (R88)
- Roberts D.H. & Sturrock P.A., 1972, ApJ 172, 435
- Ruderman M.A., Sutherland P.G., 1975, ApJ 196, 51
- Segelstein D.J., Rawley L.A., Stinebring D.R., Fruchter A.S., Taylor J.H., 1986, Nature 322, 714 (S86)
- Seiradakis J.H., et al. 1995, A&AS 111, 205 (S95)
- Shafranov V.D., 1967, Rev. of Plasma Phys., Vol.3, Consultants Bureau, New York.
- Stinebring D.R., Cordes J.M., Rankin J.M., Weisberg J.M., Boriakoff V., 1984a, ApJS 55, 247 (S84a)
- Stinebring D.R., Cordes J.M., Weisberg J.M., Rankin J.M., Boriakoff V., 1984b, ApJS 55, 279 (S84b)
- Sturrock P.A., 1971, ApJ 164, 529
- Thorsett S.E., Stinebring D.R., 1990, ApJ 361, 644 (TS90)
- Tinbergen J., 1996, Astronomical Polarimetry, Cambridge University Press
- van Ommen T.D., D'Alessandro F., Hamilton P.A. & McCulloch P.M., 1997, MNRAS 287, 307 (v97)
- Wu X.J., Manchester R.N., Lyne A.G., Qiao G.J., 1993, MNRAS 261, 630 (W93)
- Xilouris K.M., Kramer M., 1996, in Johnston S., Walker M. A. Bailes M., eds, Pulsars: Problems and Progress, IAU Colloquium 160. Astron. Soc. Pacific, San Francisco, p. 245 (XK96)
- Xilouris K.M., Rankin J.M., Seiradakis J.H., Sieber W., 1991, A&A 241,87 (X91)
- Xilouris K.M., Seiradakis J.H., Gil J., Sieber W., Wielebinski R., 1995, A&A 293, 153 (X95)
- Zepka A., Cordes J.M., Wasserman I., 1996, ApJ 456, 305 (Z96)

APPENDIX A: THE CIRCULAR POLARIZATION DATABASE

Table A1 summarizes the observed circular polarization and variation of linear position angle in mean pulse profiles for pulsars where significant circular polarization is observed. The first two columns give the pulsar J name and B name (if applicable), respectively. In the third column, the sign of $V = I_{LH} - I_{RH}$ for across the profile is indicated. Sign reversals are indicated by $+/-$ or $-/+$ and apparently distinct polarization features are indicated by repeated signs. The fourth column gives the sense of position angle variation across the profile, with ‘inc’ meaning increasing position angle (i.e. counterclockwise on the sky) and ‘dec’ meaning decreasing position angle (PA). In some cases, the variation of PA is complicated by orthogonal jumps or other reasons. Where possible, we have accounted for this in assigning a sense to the PA variation; uncertain cases are marked with ‘xx’. A few pulsars have a change in PA sense within the profile - these are marked with, e.g. ‘i+d’. The following two columns are respectively the observation frequency in MHz and the reference code, identified at the end of the Table and in the References. Comments are listed in the final column, where ‘V(f)’ means that V is a function of observation frequency, and ‘dt’ is the time resolution of the profile. For pulsars that have been observed by several authors or at different frequencies, we list each observation on a separate line. Where multiple observations at a similar frequency exist, we only list the one with the best signal/noise ratio.

Table A1. A summary of pulsar circular polarization observations

| PSR J | PSR B | V | $\langle V \rangle / S$ (%) | $\langle V \rangle / S$ (%) | σ (%) | PA | Freq. (MHz) | Ref. | Comments |
|-----------|---------|---------------------|----------------------------------|--------------------------------|-----------------|-----|----------------|------|---------------------------------------|
| 0034-0721 | 0031-07 | + | | | | dec | 268 | R83 | drifting subpulses. |
| 0133-6957 | | -+ | 10 | -3 | 3 | dec | 661 | M98 | -/+ at center of pulse |
| 0134-2937 | | - | 13 | -8 | 3 | inc | 436 | M98 | -V over profile |
| 0139+5814 | 0136+57 | + | | | | inc | 611 | LM88 | +V for only comp. $L \sim 100\%$ |
| | | + | 15 | 15 | 3 | inc | 1720 | X91 | 2 comp seen. +V near center |
| 0141+6009 | 0138+59 | + - + | | | | dec | 415 | LM88 | interesting profile |
| 0151-0635 | 0148-06 | -- | | | | inc | 611 | LM88 | -V for double cones |
| 0152-1637 | 0149-16 | + - | 12 | -2 | 1 | inc | 660 | Q95 | +V, -V for 2 comp. Large dt. $V(f)$? |
| | | (+)- | 8 | -5 | 2 | xx | 950 | v97 | no V or weak? PA not clear. |
| 0206-4028 | 0203-40 | - | 8 | -8 | 2 | xx | 660 | Q95 | good detection just at one point. |
| 0211-8159 | | - | | | | xx | 661 | M98 | -V for only high peak component |
| 0255-5304 | 0254-53 | - | 4 | -3 | 1 | xx | 950 | v97 | PA not clear, maybe dec. |
| 0304+1932 | 0301+19 | +++ | | | | dec | 430 | R83 | +V for the cones and bridge |
| | | + | | | | dec | 430 | BR80 | from individual pulses. |
| | | +++ | 10 | 10 | 2 | dec | 1400 | R89 | the same as at 430 MHz. |
| | | +++ | 12 | 12 | 3 | dec | 1720 | Mr81 | the same as 430 MHz. |
| | | +++ | 15 | 15 | 4 | dec | 2650 | Mr81 | the same as 430 MHz. |
| 0332+5434 | 0329+54 | (+) + / - | | | | dec | 1700 | B82 | both modes + / - V for core, $V(f)$ |
| | | -/+ | 13 | 10 | 3 | dec | 1720 | Mr81 | -/+ for core |
| | | -/+ | 15 | 8 | 3 | dec | 2650 | Mr81 | -/+ for core |
| | | +/- | 10 | -2 | 3 | xx | 10550 | X95 | abnormal mode: + / - V for last comp |
| 0358+5413 | 0355+54 | + - + | | | | dec | 415 | LM88 | evolves strongly with frequency |
| | | -+ | 5 | -2 | 1 | dec | 1720 | X91 | -V for 1st comp, weak +V 2nd comp |
| | | +(-+) | 11 | 9 | 3 | dec | 2650 | Mr81 | mode-changing. |
| | | -- | 14 | -14 | 2 | dec | 10550 | X95 | -V for 2 comp of both modes. |
| 0401-7608 | 0403-76 | - | 6 | -2 | 1 | dec | 1440 | Q95 | -V over profile. |
| 0437-4715 | | + - + - - / + + + | 13 | 8 | 1 | dec | 438 | N97 | complex V |
| | | - - - / + + + | 16 | -1 | 1 | dec | 661 | N97 | complex $V(f)$ |
| | | - + - + - - / + - + | 11 | -5 | 1 | dec | 1512 | N97 | complex V |
| 0452-1759 | 0450-18 | - - / + - | | | | inc | 408 | LM88 | -/+ for core, -V for cone |
| 0454+5543 | 0450+55 | + - | 12 | -6 | 2 | dec | 1700 | X91 | V for second half |
| 0459-0210 | | - | 18 | -10 | 3 | inc | 436 | M98 | -V for peak component |
| 0525+1115 | 0523+11 | -+ | | | | xx | 1400 | R89 | -V, +V for 2 comp. |
| 0528+2200 | 0525+21 | - | | | | inc | 430 | R83 | -V for one cone. Conal double |
| | | -- | 3 | -3 | 0 | inc | 1404 | S84a | -V for both cones. Best profile! |
| | | - | | | | inc | 1420 | LM88 | -V for 1st cone |
| 0536-7543 | 0538-75 | - | 8 | -5 | 1 | dec | 436 | M98 | -V over profile |
| | | - | 7 | -7 | 1 | dec | 600 | C91 | -V over profile |
| | | - | 9 | -8 | 1 | dec | 660 | Q95 | -V over profile |
| | | + - | 11 | -6 | 1 | dec | 661 | M98 | +V for first 1/3 profile, -V for rest |
| | | - | 11 | -9 | 2 | dec | 950 | v97 | similar at 800 MHz. |
| | | - | 9 | -8 | 1 | dec | 1440 | Q95 | -V over profile. |
| 0540-7125 | | -/+ | 22 | 1 | 8 | dec | 436 | M98 | -/+ at center |
| 0543+2329 | 0540+23 | - | | | | dec | 430 | BR80 | -V over profile (individual pulses) |
| | | - | | | | dec | 1400 | R89 | -V over profile. |
| | | - | | | | dec | 1720 | Mr81 | as R89 |
| | | - | | | | dec | 10550 | X95 | as R89 |
| 0601-0527 | 0559-05 | -+ | 15 | -3 | 3 | inc | 1440 | Q95 | bad s/n. -V, +V for 2 comp. |
| | | -+ | | | | inc | 1700 | X91 | as Q95 |
| 0614+2229 | 0611+22 | + | | | | inc | 409 | LM88 | $L \sim 100\%$. |
| | | + | | | | inc | 430 | RB81 | as LM88 at 409 MHz. |
| 0629+2415 | 0626+24 | -/+ | | | | dec | 1400 | R89 | -/+ for cone? |
| 0630-2834 | 0628-28 | - | | | | dec | 611 | LM88 | -V over profile. High L |
| | | - | 7 | -7 | 2 | dec | 649 | Mc78 | as LM88, but bad s/n |
| | | - | 11 | -10 | 1 | dec | 950 | v97 | as LM88 |
| | | - | 10 | -9 | 2 | dec | 1612 | Ma80 | as LM88 |
| 0631+1036 | | ++ | | | | dec | 1418 | Z96 | +V for cone? $L \sim 100\%$. |
| | | ++ | | | | dec | 1665 | Z96 | as at 1418 MHz |
| 0659+1414 | 0656+14 | (+)- | | | | dec | 1400 | R89 | +V not significant. |
| 0738-4042 | 0736-40 | - | 6 | -5 | 2 | xx | 631 | Mc78 | bad s/n and large dt. $PA(f)$? |
| | | - | 7 | -6 | 1 | inc | 950 | v97 | -V stronger and over profile |
| | | - | 7 | -6 | 1 | inc | 1612 | Ma80 | -V for one comp. |

Table A1. Continued

| PSR J | PSR B | V | $\langle V \rangle/S$ (%) | $\langle V\rangle/S$ (%) | σ (%) | PA | Freq. (MHz) | Ref. | Comments | |
|------------|----------|--------|------------------------------|-----------------------------|-----------------|------|----------------|------|---|----------------|
| 0742–2822 | 0740–28 | – | 2 | –2 | 1 | dec | 434 | M98 | weak $-V$ over profile | |
| | | – | 10 | –8 | 1 | dec | 660 | M98 | stronger $-V$ over profile | |
| | | – | 6 | –4 | 2 | dec | 800 | v97 | as 630 MHz by M78 but with bad dt | |
| | | – | 8 | –7 | 2 | dec | 950 | v97 | as 660 MHz of M98 but bad dt | |
| | | – | | | | | dec | 1420 | LM88 | $-V$ for cone? |
| | | – | 8 | –7 | 2 | dec | 1612 | Ma80 | as LM88 but with bad s/n. | |
| 0754+3231 | 0751+32 | -- | | | | inc | 1400 | R89 | $-V$ for two (conal?) comp | |
| 0758–1528 | 0756–15 | --- | 5 | –5 | 2 | inc | 1700 | X91 | weak $-V$ for two comp | |
| 0820–1350 | 0818–13 | – | 19 | –19 | 4 | xx | 631 | Mc78 | bad s/n | |
| | | – | 15 | –15 | 2 | inc | 950 | v97 | strong $-V$ for conal double? | |
| | | – | 7 | –5 | 1 | inc | 1440 | Q95 | $-V$ over profile. Bad dt | |
| 0826+2637m | 0823+26m | +/- | | | | inc | 430 | RB81 | +/- for core | |
| | | +/- | | | | inc | 1400 | R89 | +/- for core | |
| 0826+2637p | 0823+26p | – | 1 | –1 | 0 | inc | 1404 | S84a | just weak $-V$ | |
| | | + | | | | xx | 430 | RB81 | postcursor | |
| | | + | | | | xx | 1400 | R89 | strong $+V$ | |
| 0828–3417 | 0826–34 | –+ | | | | d+i | 408 | B85 | Wide profile, $-/+$ for last two comp | |
| | | + – + | | | | d+i | 610 | B85 | 1st comp is stronger & shows $+V$ | |
| 0835–4510 | 0833–45 | – | 6 | –6 | 1 | dec | 631 | Mc78 | Vela. No V at lower freq. | |
| | | – | 9 | –9 | 0 | dec | 950 | v97 | as Mc78 | |
| | | – | 14 | 14 | 1 | dec | 1612 | Ma80 | as Mc78. Best data | |
| | | -- | | | | dec | 2295 | KD83 | $-V$ for two components of Vela! | |
| 0837+0610 | 0834+06 | -- | 10 | –10 | 3 | xx | 636 | Mc78 | $-V$ for 2 comps | |
| | | +/- -- | 12 | –9 | 1 | xx | 800 | S84b | +/- for 1st comp, and $-V$ for 2nd comp | |
| | | – | 9 | –7 | 3 | inc | 950 | v97 | $-V$ only for 2nd comp | |
| | | – + – | 5 | –3 | 0 | inc | 1404 | S84a | $-V$ for comps, $+V$ for bridge. | |
| | | – + – | 8 | –7 | 2 | inc | 1612 | Ma80 | $-V$ for two comps | |
| 0837–4135 | 0835–41 | + | 27 | 27 | 2 | inc | 338 | H77 | strong $+V$ for only comp | |
| | | + | 35 | 35 | 3 | inc | 405 | H77 | strong $+V$ for only comp | |
| | | + | 20 | 20 | 1 | inc | 631 | Mc78 | as H77. Better s/n. PA not clear. | |
| | | + | 30 | 30 | 6 | xx | 800 | v97 | PA dec? V very strong | |
| | | + | 18 | 17 | 2 | dec | 950 | v97 | PA jump? V weaker | |
| | | + | 6 | 4 | 1 | inc | 1612 | Ma80 | very weak $+V$ only | |
| 0840–5332 | 0839–53 | + | 14 | 9 | 1 | inc | 660 | Q95 | $+V$ for first half profile. | |
| | | + | 15 | 10 | 4 | inc | 1440 | Q95 | $+V$ for central part, bad s/n | |
| 0846–3533 | 0844–35 | – | 19 | –16 | 3 | dec | 950 | v97 | PA dec, then flat? | |
| | | – | 12 | –8 | 2 | dec | 1440 | Q95 | $-V$ with bad s/n. | |
| 0907–5157 | 0905–51 | +(-) | 9 | 7 | 1 | inc | 660 | Q95 | $+V$ for central comp of high L | |
| | | +– | 8 | 3 | 2 | inc | 953 | v97 | + $-V$ for two comp of partial cone? | |
| 0908–4913 | 0906–49 | + | 10 | 6 | 1 | dec | 660 | Q95 | weak $+V$ for main (stronger) pulse | |
| 0922+0638 | 0919+06 | + | 9 | 7 | 2 | inc | 950 | v97 | $+V$ at strongest comp of profile | |
| | | + | 9 | 9 | 1 | inc | 1404 | S84a | $+V$ at maximum | |
| 0934–5249 | 0932–52 | + | 8 | 7 | 3 | dec | 661 | M98 | weak $+V$ over profile, bad s/n | |
| | | – | 17 | –17 | 3 | dec | 950 | v97 | $-V$ over profile, bad dt. $V(f)$? | |
| 0942–5552 | 0940–55 | – | 14 | –2 | 4 | inc | 1612 | Ma80 | $-V$ over profile, bad s/n | |
| 0942–5657 | 0941–56 | + | 17 | 12 | 3 | inc | 661 | M98 | $+V$ over profile | |
| | | + | 23 | 16 | 5 | inc | 1411 | Q95 | $+V$ for only comp. bad s/n, bad dt. | |
| 0944–1354 | 0942–13 | –/+ | 22 | 14 | 2 | dec | 409 | LM88 | core? Two comp at 1.42GHz (see S95) | |
| 0946+0951 | 0943+10 | + | | | | dec | 430 | RB81 | $+V$ for the only comp | |
| 0953+0755m | 0950+08m | – | | | | dec | 800 | S84b | weak $-V$ for second half profile | |
| | | – | 8 | –6 | 0 | dec | 950 | v97 | $-V$ over profile | |
| | | – | | | | dec | 1400 | R89 | weak V . $V(f)$? | |
| | | – | 6 | –6 | 1 | dec | 1404 | S84a | $-V$ for whole profile. | |
| | | – | 9 | –9 | 1 | xx | 1612 | Ma80 | worse s/n than S84a. | |
| 0953+0755 | 0950+08i | –+ | | | | dec | 1400 | R89 | bad s/n | |
| 0955–5304 | 0953–52 | + | 13 | 11 | 2 | xx | 661 | M98 | $+V$ for strongest central component | |
| 1001–5507 | 0959–54 | +/- | 4 | 2 | 1 | inc | 654 | M98 | weak +/- for core, but PA not clear | |
| | | +/- | 5 | 2 | 3 | inc | 950 | v97 | as 654MHz but bad s/n | |
| 1034–3224 | | +/- | | | | xx | 436 | M98 | +/- for strongest of more than 6 comp! | |
| 1123–4844 | | + | 18 | 13 | 5 | dec? | 436 | M98 | $+V$ strong between comps | |

Table A1. Continued

| PSR J | PSR B | <i>V</i> | $\langle V \rangle/S$ (%) | $\langle V\rangle/S$ (%) | σ (%) | PA | Freq. (MHz) | Ref. | Comments |
|-----------|---------|----------|------------------------------|-----------------------------|-----------------|-----|----------------|------|--|
| 1136+1551 | 1133+16 | -- | 15 | -15 | 2 | inc | 638 | Mc78 | - <i>V</i> for two comps and bridge! |
| | | -- | 8 | -5 | 4 | inc | 950 | v97 | bad s/n for - <i>V</i> |
| | | -- - | 8 | -8 | 1 | inc | 1404 | S84a | - <i>V</i> is complicated for 1st comp. |
| | | -- | 10 | -10 | 1 | inc | 1612 | Ma80 | as Mc78. |
| 1157-6224 | 1154-62 | + | 20 | 17 | 5 | dec | 631 | Mc78 | bad s/n for <i>V</i> |
| | | + | 15 | 12 | 4 | dec | 950 | v97 | + <i>V</i> for second part of profile |
| 1202-5820 | 1159-58 | + | 10 | 9 | 2 | inc | 436 | M98 | + <i>V</i> over profile |
| 1210-5559 | | - | 8 | -7 | 2 | xx | 436 | M98 | - <i>V</i> over profile, bad dt |
| 1224-6407 | 1221-63 | + | 32 | 15 | 7 | inc | 631 | Mc78 | bad s/n, strong <i>V</i> |
| | | + | 33 | 26 | 5 | inc | 950 | v97 | Strong + <i>V</i> |
| | | + | 14 | 13 | 4 | inc | 1560 | W93 | s/n for <i>V</i> just ok, but large dt. |
| | | + | 20 | 20 | 3 | inc | 1612 | Ma80 | <i>V</i> is much weaker |
| 1239+2453 | 1237+25 | ++/- | | | | dec | 408 | LM88 | +/- for core |
| | | +++/-- | | | | dec | 410 | M71 | +/- for core, + <i>V</i> for two conal comp |
| | | -/+/- | | | | xx | 430 | B82 | normal mode, but +++ for abnormal mode |
| | | +++/- | 13 | 4 | 1 | dec | 1404 | S84a | <i>V</i> for cone & core |
| | | +++/-- | | | | dec | 1700 | B82 | same <i>V</i> for both modes |
| 1243-6423 | 1240-64 | +/- | 13 | 0 | 4 | xx | 2700 | Mr81 | |
| | | + | 19 | 18 | 2 | inc | 631 | Mc78 | + <i>V</i> for only comp |
| | | + | 9 | 8 | 3 | inc | 800 | v97 | weaker + <i>V</i> |
| | | -/+ | 6 | 3 | 2 | inc | 950 | v97 | weaker -/+ + <i>V</i> , PA varies |
| 1253-5820 | | - | 13 | -13 | 2 | inc | 1612 | Ma80 | only - <i>V</i> , stronger |
| | | + | 15 | 10 | 3 | inc | 436 | M98 | + <i>V</i> over profile |
| 1302-6350 | 1259-63 | + | 13 | 11 | 2 | dec | 1520 | MJ95 | + <i>V</i> seen from one of two comp |
| | | + | 18 | 12 | 3 | dec | 4680 | MJ95 | as at 1520 MHz |
| 1320-5359 | 1317-53 | - | 7 | -5 | 7 | dec | 600 | C91 | weak - <i>V</i> over profile |
| 1326-5859 | 1323-58 | -+ | 11 | 6 | 2 | dec | 950 | v97 | -/+ for core |
| 1328-4357 | 1325-43 | -+ | 10 | 5 | 2 | inc | 436 | M98 | -/+ for first two of 3 comp |
| 1328-4921 | 1325-49 | +/- | 18 | 0 | 6 | xx | 436 | M98 | +/- near centre |
| 1338-6204 | 1334-61 | + | 10 | 6 | 2 | i+d | 1440 | Q95 | weak + <i>V</i> in central part |
| 1341-6220 | 1338-62 | - | 25 | -12 | 9 | inc | 1411 | Q95 | bad s/n for - <i>V</i> . <i>L</i> ~90%. |
| 1357-6228 | 1353-62 | - | 16 | 12 | 5 | dec | 1612 | Ma80 | bad s/n for - <i>V</i> over profile |
| 1359-6038 | 1356-60 | + | 22 | 22 | 2 | inc | 660 | M98 | + <i>V</i> over profile, <i>L</i> ~ 100% |
| | | + - | 15 | 4 | 4 | inc | 1560 | W93 | bad s/n for - <i>V</i> and bad dt |
| 1453-6413 | 1449-64 | ++ | 11 | 9 | 1 | inc | 400 | H77 | + <i>V</i> varies with freq.? |
| | | ++ | 6 | 5 | 2 | inc | 950 | v97 | 3 components? |
| 1456-6843 | 1451-68 | -/+ | 8 | 4 | 1 | dec | 400 | H77 | -/+ for core, same at 271 MHz (R83). |
| | | --/++ | 6 | 0 | 1 | dec | 649 | Mc78 | as at 400 MHz, -/+ at centre |
| | | --/++ | 6 | 3 | 0 | dec | 950 | v97 | two comp in core |
| | | --/++ | 7 | -1 | 1 | dec | 1612 | Ma80 | symmetric <i>V</i> ? |
| 1509+5531 | 1508+55 | +/- | | | | dec | 610 | LM88 | +/- over triple profile |
| | | ++/- | 8 | 0 | 2 | dec | 1612 | Mr81 | as 610 MHz |
| 1527-3931 | 1524-39 | + | 18 | 8 | 6 | dec | 436 | M98 | + <i>V</i> for conal double, bad s/n |
| | | + | 20 | 13 | 5 | dec | 661 | M98 | as at 436 MHz |
| 1527-5552 | 1523-55 | -/+ | 20 | 13 | 2 | dec | 661 | M98 | -/+ for the core? |
| 1534-5334 | 1530-53 | +/- | | | | dec | 960 | v97 | +/- for the first strong comp |
| | | +/- | 8 | -4 | 2 | dec | 1612 | Ma80 | as v97, partial cone? |
| 1537+1155 | 1534+12 | --/+ | | | | dec | 430 | A96 | +/- for main comp, MSP |
| 1542-5304 | | + | 16 | 10 | 5 | inc | 661 | M98 | + <i>V</i> in 2nd half of profile |
| 1543+0929 | 1541+09 | +++ | | | | d+i | 430 | R83 | possible 7 comp, strong - <i>V</i> at centre |
| | | +++ | 13 | -1 | 2 | d+i | 1400 | R89 | <i>V</i> seen over the very wide profile. |
| 1544-5308 | 1541-52 | --/++ | 11 | 1 | 2 | xx | 661 | M98 | -/+ for central comp |
| 1557-4258 | | - | 13 | -8 | 2 | dec | 661 | M98 | - <i>V</i> for central comp with strong <i>L</i> |
| 1559-4438 | 1556-44 | - | 12 | -12 | 2 | dec | 631 | Mc78 | <i>L</i> ~ 60% |
| | | -+ | 5 | 3 | 1 | dec | 661 | M98 | <i>V</i> variable? |
| | | - | 8 | -7 | 4 | dec | 800 | v97 | weaker <i>V</i> |
| | | - | 13 | -10 | 3 | dec | 950 | v97 | - <i>V</i> stronger |
| | | -/+ | 11 | -8 | 1 | dec | 1490 | M98 | resolved profile with interesting <i>V</i> |
| | | - | 8 | -4 | 3 | dec | 1560 | W93 | weak - <i>V</i> . |
| | | - | 16 | -15 | 2 | dec | 1612 | Ma80 | - <i>V</i> at centre |

Table A1. Continued

| PSR J | PSR B | V | $\langle V \rangle/S$ (%) | $\langle V\rangle/S$ (%) | σ (%) | PA | Freq. (MHz) | Ref. | Comments |
|-----------|----------|----------|------------------------------|-----------------------------|-----------------|-----|----------------|------|---|
| 1600–5044 | 1557–50 | + | 21 | 20 | 5 | inc | 950 | v97 | bad s/n, scattering |
| | | + | 16 | 14 | 2 | inc | 1560 | W93 | bad dt, +V in part of profile |
| | | + | 23 | 21 | 4 | inc | 1612 | Ma80 | as W93. |
| 1604–4909 | | +/- | 6 | 3 | 1 | inc | 661 | M98 | +/- for core |
| 1607–0032 | 1604–00 | -/+ ++ | | | | dec | 430 | R88 | -/+ for one comp, +V for another comp |
| | | - | 9 | -7 | 2 | xx | 631 | Mc78 | -V over most of profile |
| | | + - + | | | | xx | 1400 | R89 | +V doubtful, -V OK |
| 1614–5047 | 1610–50 | + | 26 | 10 | 12 | dec | 1411 | Q95 | bad dt |
| 1633–5015 | 1629–50 | - | 18 | -13 | 3 | inc | 1411 | Q95 | strong -V over profile |
| 1635+2418 | 1633+24 | -(+) | | | | dec | 1400 | R89 | -V for central comp |
| 1644–4559 | 1641–45 | - | 3 | -2 | 0 | inc | 950 | v97 | weak -V over scattered profile |
| | | (-) + - | 4 | -1 | 1 | inc | 1612 | Ma80 | +V for peak. |
| 1646–6831 | 1641–68 | +(-) | 12 | 5 | 1 | i+d | 660 | Q95 | +V at centre |
| | | +(-) | 14 | 5 | 3 | i+d | 953 | v97 | bad s/n for -V, PA = inc+dec? |
| 1645–0317 | 1642–03 | +/- | | | | xx | 408 | LM88 | complicated PA |
| | | - | | | | xx | 410 | M71 | -V over profile |
| | | - | 8 | -7 | 1 | inc | 631 | Mc78 | -V for the only comp, V(f)? |
| | | - | 3 | -2 | 1 | dec | 950 | v97 | -V for the only comp, PA(f)? |
| 1651–4246 | 1648–42 | - | 19 | -13 | 4 | dec | 950 | v97 | -V for 2nd part of profile, bad s/n. |
| | | - | 11 | -3 | 4 | dec | 1560 | W93 | as at 950 MHz, better s/n |
| 1700–3312 | | - | 27 | -24 | 8 | inc | 434 | M98 | -V over profile, but with bad s/n |
| 1703–3241 | 1700–32 | -/+ | 7 | -1 | 2 | inc | 950 | v97 | -/+ for core |
| | | -/+ | 10 | -2 | 3 | inc | 1612 | Ma80 | -/+ for core seen at 409MHz (LM88). |
| 1705–1906 | 1702–19m | - | 60 | -60 | 3 | dec | 408 | B88 | large -V over whole profile |
| 1705–1906 | 1702–19i | - | 60 | -60 | 3 | dec | 408 | B88 | also large -V |
| 1709–4428 | 1706–44 | - | 17 | -16 | 3 | inc | 1440 | Q95 | -V over only comp, L up to 90%. |
| 1713+0747 | | -/+ | | | | i+d | 1400 | XK96 | -/+ for core? PA inc+dec? |
| 1721–3532 | 1718–35 | - | 17 | -14 | 4 | dec | 1411 | Q95 | -V appears at strongest part of profile |
| 1722–3712 | 1719–37 | + | 9 | 8 | 2 | inc | 661 | M98 | weak +V over profile, high L |
| 1731–4744 | 1727–47 | + | 9 | 7 | 3 | xx | 400 | H77 | bad s/n and PA not clear |
| | | + | 5 | 4 | 1 | dec | 800 | v97 | weak +V for 1st comp. Same at 950 MHz |
| 1740–3015 | 1737–30 | - | 20 | -19 | 2 | dec | 660 | Q95 | -V over profile, bad dt & bad s/n |
| | | - | 22 | -22 | 3 | dec | 1560 | W93 | -V strong at 2nd half of only comp. |
| 1740+1311 | 1737+13 | ++/- | | | | dec | 430 | R88 | +/- for core & +V for cone |
| | | ++ +/- | | | | dec | 1400 | R89 | as R88 |
| 1741–3927 | 1737–39 | + | 7 | 4 | 1 | xx | 661 | M98 | weak +V over profile |
| | | + | 10 | 7 | 3 | inc | 954 | v97 | +V at centre, bad dt |
| 1745–3040 | 1742–30 | - | 10 | -9 | 3 | xx | 950 | v97 | PA and V similar to X91 |
| | | - - - | 15 | -15 | 2 | xx | 1700 | X91 | -V for 3 (conal?) comp |
| 1751–4657 | 1747–46 | -/+ ++ | 12 | 8 | 1 | dec | 436 | M98 | -/+ for 1st comp, 2nd comp +V |
| | | + | 8 | 6 | 1 | dec | 631 | Mc78 | +V at center |
| | | -/+ ++ | | | | dec | 950 | v97 | as M98 at 1522MHz. |
| 1752–2806 | 1749–28 | -/+ ++ | 9 | 6 | 2 | dec | 1522 | M98 | same as 436 MHz |
| | | - | 7 | -7 | 1 | xx | 631 | Mc78 | bad dt, V(f)? |
| | | - | 3 | -2 | 0 | dec | 950 | v97 | V(f), PA(f) |
| | | -(/+) | 5 | 1 | 1 | xx | 1612 | Ma80 | weak +V, bad dt. |
| | | -/+ | 5 | 0 | 3 | xx | 1720 | Mr81 | -/+ for core? |
| | | -/+ | 13 | 11 | 3 | dec | 2650 | Mr81 | -/+ for core? 3 comp? |
| 1801–0357 | | +/- | 20 | -6 | 4 | dec | 661 | M98 | +/- for core, but PA not clear |
| 1803–2137 | 1800–21 | ++ | 21 | 20 | 3 | dec | 1560 | W93 | interesting profile with high L |
| 1807–0847 | 1804–08 | + - - | 10 | 0 | 2 | xx | 1700 | X91 | very weak V for central and last comp |
| 1817–3618 | 1813–36 | - | 13 | -10 | 1 | xx | 660 | Q95 | strong -V over part profile, bad dt |
| 1820–0427 | 1818–04 | - | | | | xx | 410 | M71 | -V over part profile |
| | | - | 18 | -12 | 4 | inc | 631 | Mc78 | poor s/n |
| | | - | 13 | -6 | 3 | inc | 950 | v95 | better s/n |
| 1823+0550 | 1821+05 | ++ / - - | 11 | 2 | 2 | dec | 1400 | R89 | +/- for core, PA not clear |
| 1829–1751 | 1826–17 | - | 19 | -17 | 2 | xx | 436 | M98 | strong -V, scattered profile. Flat PA |
| | | - | 15 | -11 | 2 | d+i | 660 | M98 | strong -V over profile, PA= dec+inc! |
| | | - | 17 | -11 | 5 | xx | 950 | v97 | PA inc+dec? |
| 1836–1008 | 1834–10 | -+ | 10 | -3 | 3 | dec | 1720 | X91 | weak -/+ at pulse center. poor s/n |
| 1841+0912 | 1839+09 | + - + | 5 | -3 | 1 | dec | 1400 | R89 | + - + for 3 comp, +V very weak. |
| 1848–1952 | 1845–19 | - | 14 | -13 | 5 | xx | 950 | v97 | -V for 1st resolved component |

Table A1. Continued

| PSR J | PSR B | V | $\langle V \rangle/S$ (%) | $\langle V\rangle/S$ (%) | σ (%) | PA | Freq. (MHz) | Ref. | Comments |
|------------|----------|---------|------------------------------|-----------------------------|-----------------|-----|----------------|------|--|
| 1852–2610 | | + | 9 | 2 | 3 | dec | 436 | M98 | strong L , weak V |
| 1857+0943 | 1855+09m | +- | | | | dec | 1400 | S86 | +/- V for 2 comp. |
| 1900–2600 | 1857–26 | +/- | | | | xx | 170 | R83 | +/- for core comp |
| | | +/- -- | | | | xx | 268 | R83 | +/- for core comp |
| | | ++ / -- | 17 | -3 | 4 | dec | 631 | Mc78 | +/- for central part |
| | | +/- | 12 | 2 | 2 | dec | 661 | M98 | +/- for central part |
| | | +/- | 12 | -1 | 1 | dec | 950 | v97 | +/- for central part |
| | | +/- | 16 | -2 | 1 | dec | 1490 | M98 | +/- for central part |
| | | ++ / -- | 20 | -1 | 3 | dec | 1612 | Ma80 | +/- over most of profile |
| | | +/- | 22 | 0 | 4 | dec | 2650 | Mr81 | |
| 1901+0331 | 1859+03 | +/- | 12 | 3 | 2 | dec | 1400 | R89 | +/- for core |
| 1903+0135 | 1900+01 | + | 13 | 8 | 4 | inc | 950 | v97 | + V for central comp only |
| 1907+4002 | 1905+39 | -- | 10 | -10 | 3 | dec | 1700 | X91 | - V for 2 comp, s/n just ok. |
| 1909+0254 | 1907+02 | -/+ | | | | dec | 430 | RB81 | triple at 1410 MHz (S95) |
| 1910+0358 | 1907+03 | (-+)- | 16 | -13 | 2 | dec | 1400 | R89 | strong - V from 2nd half profile. |
| 1909+1102 | 1907+10 | - | 12 | -12 | 2 | inc | 1400 | R89 | - V for core only? |
| 1910+1231 | 1908+12 | + | | | | xx | 430 | RB81 | s/n for + V just ok |
| 1912+2104 | 1910+20 | - | | | | inc | 1400 | R89 | s/n for - V just ok |
| 1913–0440 | 1911–04 | +- + | 15 | -1 | 4 | xx | 400 | H77 | bad s/n for V |
| | | +- | 8 | -5 | 2 | inc | 950 | v97 | +/- for two unresolved comp? |
| 1913+1400 | 1911+13 | + - (+) | | | | xx | 1400 | R89 | bad s/n for + V . PA=dec? |
| 1915+1009 | 1913+10 | + | 40 | 40 | 2 | d+i | 1400 | R89 | very strong + V over profile |
| 1915+1606 | 1913+16 | -/+ ++ | | | | inc | 430 | C90 | -/+ for 1st comp |
| 1915+1647 | 1913+167 | + | | | | dec | 430 | RB81 | + V at centre |
| | | +/- | | | | xx | 1400 | R89 | two core comps |
| 1916+0951 | 1914+09 | - | | | | dec | 430 | RB81 | - V for 1st comp |
| | | + | | | | dec | 1400 | R89 | weak + V over profile |
| 1916+1312 | 1914+13 | - | 37 | -37 | 2 | inc | 1400 | R89 | very strong - V over profile |
| 1917+1353 | 1915+13 | - | | | | dec | 430 | RB81 | - V for only comp |
| | | - | | | | dec | 1400 | R89 | - V over profile |
| 1918+1444 | 1916+14 | + | | | | xx | 430 | RB81 | bad s/n |
| | | + | | | | dec | 1400 | R89 | + V over profile |
| 1919+0021 | 1917+00 | + | | | | xx | 418 | RB81 | + V for core |
| | | ++ - | | | | inc | 1400 | R89 | triple profile, +/-? |
| 1921+1419 | 1919+14 | +- | | | | dec | 430 | RB81 | + V weak, - V strong. |
| | | +- | | | | dec | 1400 | R89 | - V not so strong |
| 1922+2110 | 1920+21 | + | 20 | 3 | 2 | dec | 430 | RB81 | + V for core? bad dt. |
| 1926+1648 | 1924+16 | -/+ | | | | inc | 430 | RB81 | -/+? high L |
| | | + | | | | inc | 1400 | R89 | weak + V over profile |
| 1932+1059m | 1929+10m | -- | | | | dec | 430 | BR80 | - V for all comps, $L \sim 100\%$ |
| | | ++ -- | 2 | 0 | 0 | dec | 800 | S84b | V very weak, +/- V for central comp. |
| | | -- | | | | dec | 1400 | R89 | weaker - V for 2 or 3 comp. |
| | | -- | 1 | -1 | 0 | dec | 1404 | S84a | weaker - V for 3 comp. |
| | | -- | | | | dec | 1665 | P90 | - V for all at 1665 and 430 MHz. |
| | | ++ | | | | dec | 1700 | X91 | very weak + V for all |
| 1932+1059m | 1929+10i | - | | | | inc | 430 | RB81 | - V for main comp |
| | | - | | | | xx | 1400 | R89 | - V for core? |
| | | - | | | | inc | 1665 | P90 | - V for all at 430 and 1665 MHz. |
| 1932–3655 | | +/- | 22 | 9 | 8 | inc | 658 | M98 | significant +/- V for the peak comp |
| 1935+1616 | 1933+16 | -/+ | | | | xx | 430 | R83 | -/+ for core |
| | | -/+ | 15 | -1 | 1 | xx | 1440 | R89 | -/+ for two core comps |
| | | -/+ | 14 | 0 | 3 | xx | 1720 | Mr81 | good s/n |
| | | -/+ | 15 | 0 | 3 | xx | 2700 | Mr81 | -/+ for core |
| 1939+2134m | 1937+21m | - | | | | xx | 1418 | TS90 | across whole pulse |
| 1939+2134i | 1937+21i | - | | | | xx | 1418 | TS90 | |
| 1941–2602 | 1937–26 | - | 13 | -7 | 5 | dec | 1560 | W93 | weak - V , s/n just ok |
| 1946+1805 | 1944+17 | -(+) -- | 5 | 4 | 1 | inc | 1404 | S84a | V over profile |
| 1946+2244 | 1944+22 | - | | | | xx | 430 | RB81 | s/n just ok |
| 1946–2913 | 1943–29 | + | 15 | 9 | 6 | inc | 434 | M98 | + V just for central strong comp |
| 1948+3540 | 1946+35 | + | | | | xx | 430 | RB81 | + V for scattered profile |
| | | ++ | | | | inc | 1400 | R89 | + V for 2 or 3 comp |

Table A1. Continued

| PSR J | PSR B | V | $\langle V \rangle/S$ (%) | $\langle V\rangle/S$ (%) | σ (%) | PA | Freq. (MHz) | Ref. | Comments |
|------------|----------|----------|------------------------------|-----------------------------|-----------------|-----|----------------|------|---|
| 1954+2923 | 1952+29 | --+- | | | | inc | 430 | RB81 | strong $-V$ |
| | | ---+- | 21 | -19 | 2 | de? | 1400 | R89 | $-V$ over most of profile |
| 1959+2048m | 1957+20m | (+)/- | | | | xx | 430 | TS90 | MSP. very weak L |
| | | -/+ | | | | xx | 430 | F90 | V appears to be reversed to TS90. |
| 1959+2048i | 1957+20i | +- | | | | xx | 430 | TS90 | as main pulse |
| | | -+ | | | | xx | 430 | F90 | as main pulse |
| 2004+3137 | 2002+31 | +/- | | | | xx | 430 | RB81 | +/- for core, bad dt. |
| | | +/- | 4 | 0 | 1 | inc | 1400 | R89 | PA is not so clear. |
| 2006-0807 | 2003-08 | -+ / -- | 14 | -11 | 2 | inc | 1700 | X91 | +/- core, $-V$ for cone |
| 2018+2839 | 2016+28 | - | 6 | -6 | 1 | inc | 1404 | S84a | $-V$ for central part |
| 2022+2854 | 2020+28 | +/- --- | | | | inc | 430 | C78 | But also show -- for two cones! |
| | | +/- --- | 8 | -7 | 0 | inc | 800 | S84b | +/- for 1st comp |
| | | +/- --- | 7 | -7 | 0 | inc | 1404 | S84a | as at 800 MHz, but +/- weak |
| 2022+5154 | 2021+51 | - | 4 | -4 | 1 | inc | 10550 | X95 | weak $-V$ |
| 2021+2145 | 2025+21 | + | | | | dec | 430 | RB81 | s/n just ok |
| 2030+2228 | 2028+22 | ++ | | | | dec | 1400 | R89 | weak $+V$ for 2 comps |
| 2046-0421 | 2043-04 | - | | | | xx | 950 | v97 | $-V$ for strongest comp |
| 2046+1540 | 2044+15 | +++ | | | | i+d | 1400 | R89 | very weak $+V$ for 2 comp |
| 2048-1616 | 2045-16 | +++ | 7 | 3 | 1 | dec | 950 | v97 | $+V$ for outer conal comps |
| | | ++ / - + | | | | dec | 1420 | LM88 | weak +/- for core, $+V$ for conal comps |
| 2053-7200 | 2048-72 | +- | 13 | -4 | 1 | inc | 660 | Q95 | + $-V$ for 2 comp with bad s/n. |
| | | +/- | 8 | -2 | 2 | inc | 661 | M98 | confirm + $-V$ seen by Q95 |
| | | +- | | | | inc | 950 | v97 | + $-V$ for two comps |
| | | -+ | 10 | -5 | 2 | inc | 1440 | Q95 | bad s/n for V , $V(f)$? |
| 2055+3630 | 2053+36 | - | | | | xx | 1400 | R89 | bad s/n |
| 2113+2754 | 2110+27 | -- | | | | dec | 1400 | R89 | weak V |
| 2113+4644 | 2111+46 | +/- | | | | dec | 610 | LM88 | +/- for core |
| | | +/- | 10 | 0 | 3 | dec | 1720 | Mr81 | also 2650 MHz. |
| 2116+1414 | 2113+14 | +/- | | | | inc | 1400 | R89 | +/- at centre but not peak |
| 2144-3933 | | -/+ | 17 | 3 | 2 | inc | 661 | M98 | -/+ for core |
| 2145-0750 | | -+ | | | | in? | 1400 | XK96 | PA variation not clear. |
| 2155-3118 | 2152-31 | + | 25 | 22 | 7 | de? | 950 | v97 | Strong $+V$, weak L |
| 2219+4754 | 2217+47 | + | | | | inc | 1612 | Mr81 | but at 2650 MHz, weak $-V$? |
| 2225+6535 | 2224+65 | -- | | | | dec | 408 | LM88 | $-V$ for 2 comps, bad s/n, PA=dec+flat |
| 2305+3100 | 2303+30 | ++ | | | | inc | 1400 | R89 | weak $+V$ over comp, good s/n |
| 2313+4253 | 2310+42 | -+- | 13 | -11 | 1 | inc | 1700 | X91 | V over profile |
| 2317+2149 | 2315+21 | - | | | | inc | 409 | LM88 | core? bad dt. bad s/n |
| | | --- | | | | xx | 1400 | R89 | $-V$ varies for 2 (or 3) comp |
| 2324-6054 | 2321-61 | + | 13 | 11 | 1 | dec | 660 | Q95 | $+V$ for 1 of 2 (conal) comp |
| | | +(-) | | | | dec | 950 | v97 | bad s/n for V |
| 2330-2005 | 2327-20 | -- | 22 | -22 | 1 | inc | 648 | Mc78 | strong $-V$ over whole profile |
| | | -- | 12 | -11 | 1 | inc | 950 | v97 | weaker $-V$, good s/n |
| 2346-0609 | | + | 11 | 9 | 2 | dec | 436 | M98 | conal double, $+V$ for second comp |
| 2354+6155 | 2351+61 | ++ | 9 | 9 | 3 | dec | 1700 | X91 | $+V$ for two comp |

References: Manchester 1971 (M71); Hamilton et al. 1977 (H77); Cordes, Rankin & Backer 1978 (C78); McCulloch et al. 1978 (Mc78); Backer & Rankin 1980 (BR80); Manchester, Hamilton & McCulloch 1980 (Ma80); Morris et al. 1981 (Mr81); Rankin & Benson 1981 (RB81); Barter et al. 1982 (B82); Krishnamohan & Downs 1983 (KD83); Rankin 1983 (R83); Stinebring et al. 1984a (S84a); Stinebring et al. 1984b (S84b); Biggs et al. 1985 (B85); Segelstein et al. 1986 (S86); Biggs et al. 1988 (B88); Lyne & Manchester 1988 (LM88); Rankin, Wolszczan & Stinebring 1988 (R88); Rankin, Stinebring & Weisberg 1989 (R89); Cordes, Wasserman & Blaskiewicz 1990 (C90); Fruchter et al. 1990 (F90); Phillips 1990 (P90); Thorsett & Stinebring 1990 (TS90); Costa et al. 1991 (C91); Xilouris et al. 1991 (X91); Wu et al. 1993 (W93); Gould 1994 (G94); Manchester & Johnston 1995 (MJ95); Qiao et al. 1995 (Q95); Seiradakis et al. 1995 (S95); Xilouris et al. 1995 (X95); Arzoumanian et al. 1996 (A96); Xilouris & Kramer 1996 (XK96); Zepka, Cordes & Wasserman 1996 (Z96); Navarro et al. 1997 (N97); van Ommen et al. 1997 (v97); Manchester, Han & Qiao 1998 (M98).